

A Prototype of Wireless Power and Data Acquisition System for Large Detectors

P. De Lurgio^a, Z. Djurcic^a, G. Drake^a, R. Hashemian^b, A. Kreps^a, M. Oberling^a, T. Pearson^b, H. Sahoo^a

^aArgonne National Laboratory, Argonne, IL 60439, USA

^bNorthern Illinois University, Dekalb, IL 60115, USA

Abstract

A new prototype wireless data acquisition system has been developed with the intended application to read-out instrumentation systems having a large number of channels. In addition such system could be deployed in smaller detectors requiring increased mobility. The data acquisition and control system is based on 802.11n compliant hardware and protocols. In this paper we describe our case study with a single readout channel performed for a potential large detector containing photomultiplier tubes. The front-end circuitry, including a high-voltage power supply is powered wirelessly thus creating an all-wireless detector readout. The benchmarked performance of the prototype system and how a large scale implementation of the system might be realized are discussed.

Keywords: Wireless communications, RF, Optical

1. Introduction

The goal of this R&D project was to build a detector module that operates from wireless power and sends data wirelessly. The motivation is the elimination of the massive cable plants that are typical of large detectors, which can result in cost reductions, simplified installation and repair, and reductions in detector dead mass. Specially, cabling is not practical for detectors in remote locations or hostile environments. The primary purpose of the effort described here is to ascertain the feasibility and practicality of such devices as single detector modules configured as arrays in a large detector. We chose a photomultiplier tube (PMT) as the basis for this study, in

part because of ubiquity of PMTs in high energy physics detectors, as well as the compact nature of the detector. In particular we selected a 10 inch diameter PMT, a Hamamatsu R7081 [1], which has a dark noise rate of ~ 10 kHz. The system specifications include the capability to measure single photoelectrons, which imposes requirements on bandwidth and sensitivity of the instrumentation. Such requirements are often listed in connection with large neutrino detectors and include examples of considered water-based LBNE [2], MEMPHYS [3], Hyper-K [4], and CHIPS [5] detectors. Detectors used for homeland security also use some of these technologies and techniques. Simplifying the implementation of large detectors with high channel counts will facilitate optimized detection of nuclear materials and other contra-band. Numerous additional applications could benefit from infrastructure simplification, increased mobility, and stand-off distance capability of wireless techniques. Some examples of these include monitoring of the neutrino flux at a nuclear reactor, large mobile neutron detectors for detection of radioactive material in security applications, and detectors operating in high-radiation areas. Operation in real world conditions requires the ability for detectors to be easily relocated, and the ability to operate continuously for long periods of time, both of these are improved using low-power wireless techniques. For neutrino and other low-rate experiments, the single photoelectron rate dominates the event rate. If we assume for each event that the data would be comprised of 6 bytes, 2 bytes of pulse height information and a 4 byte timestamp, at 10 kHz, this translates to 60 kB, or 480 kb/s. For a single detector element, these data rates are achievable for a wireless readout. Extrapolating to a large detector with tens of thousands of channels translates into a data rate on the order of ~ 20 Gb/s, which is quite challenging for wireless readout. The target specifications for the prototype system are summarized in Table 1.

Successful demonstration of an all wireless system could be transformational when realized in a practical, cost effective, and reliable fashion. This prototyping work could in principle, with more design effort, allow for applications of these new read-out technologies.

2. Design Considerations

The R&D project began by researching the different technologies for wireless data and power transmission. For wireless data transmission, two techniques in use today, radio frequency (RF) wireless and free-space optical

Table 1: Target specifications for the wireless data acquisition system.

Specification	Target
Maximum event rate (single p.e.)	10 kHz
Bytes per event	6 (2 pulse height, 4 time-stamp)
Average data rate per front-end channel	60 kB/s
Total power consumption @ 10 kHz	250 mW
Digital	120 mW
Front-end	30 mW
HV	80 mW
Data transfer rate	35 Mb/s
Bit error rate	$< 1 \times 10^{-12}$
Additional Features	Self-trigger for pedestals Data pull Programmable HV Programmable Discriminator

were considered. Similarly, for wireless power transmission RF and optical were considered as well. Other methods of transmitting power wirelessly; for example, through strongly coupled magnetic resonances [6] were considered. In selecting technologies, a preference was placed on the use of inexpensive, off-the-shelf technologies that could be implemented relatively easily, with minimal risk and which could meet the performance goals of this project.

2.1. Wireless Data Transmission

For wireless data transmission, optical links support higher data rates than RF. Individual free space links over distances of meters can achieve transfer rates of approximately 1 Gb/s [7]. However, RF transmission does not require line-of-sight, and an individual transmitter can communicate with many front-ends. RF data transmission was chosen for this project because both of these advantages provide significant simplification and cost reduction. The difficulty with RF is that the bandwidth of an individual link is typically modest, approximately 100 MB/s, and the available RF bandwidth is shared by all elements of the detector.

There are two primary categories of wireless data technologies in use today. These are mobile/cellular, and wireless local area network (WLAN). Each has different variants for specific applications. For this project, we focused on WLAN technologies, since they have the highest data throughput.

Of the different WLAN variants, we selected 802.11n, since at the time, it offered the highest data throughput and has sufficient range for this application. Combined with the ubiquity of hardware and the relative ease of implementation, made this technology the preferred option. The total data rate of a single stream 802.11n link is approximately 65 Mb/s [8]. Note that this is the total data rate and not the payload data rate, which is ~ 35 Mb/s. This is sufficient for our single prototype front-end. However, for a large detector, the challenge would be in transferring data from thousands of readout channels over a limited and common frequency spectrum.

One frequency range in 802.11n is centered in the U-NII and ISM bands at about 5.5 GHz. It has an overall bandwidth of approximately 1.2 GHz from about 4.9 GHz to 6.1 GHz. This ignores limitations imposed by the governing agencies that dictate the use of the electromagnetic spectrum. Under certain circumstances, the full spectrum can be available for use with dynamic frequency selection capable devices [9]. The approach uses a large number of access points in a large detector system to accommodate the total payload data rate needed by the data acquisition system. Single stream 802.11n access points can have an individual operating bandwidth of 20 MHz or 40 MHz. With 20 MHz wide channels, it should be possible to populate the 1.2 GHz frequency with up to 48 access points. For a single stream 802.11n link this translates into a total payload data rate of 1.68 Gb/s, as illustrated in Figure 1 below. The system consists of many access points (~ 48) each communicating to many clients (~ 64), for a total of 3072 clients. This assumes 480 kb/s per front-end and a burst transfer rate of 35 Mb/s.

For a large detector with tens of thousands of channels, this payload data rate is clearly insufficient. There are two extensions of this concept to increase the data throughput. First, the use of directional antennas and the intrinsic shielding created by the detector volume should allow the same frequency range to be utilized in different locations on the detector. This effectively multiplies the usable spectrum, where the limits would depend on the particular detector geometry. Second, the 802.11n standard includes extensions that allow for multiple input and output (MIMO) wireless streams. This extension could significantly increase data throughput. For example, a 4×4 MIMO implementation supports 4 simultaneous transmit and receive streams to yield a data throughput of 600 Mb/s, which translates into a maximum payload data rate of 320 Mb/s. However, 4×4 MIMO requires 40 MHz wide channels, which means the 1.2 GHz frequency band would support approximately 24 access points. This translates into a much higher

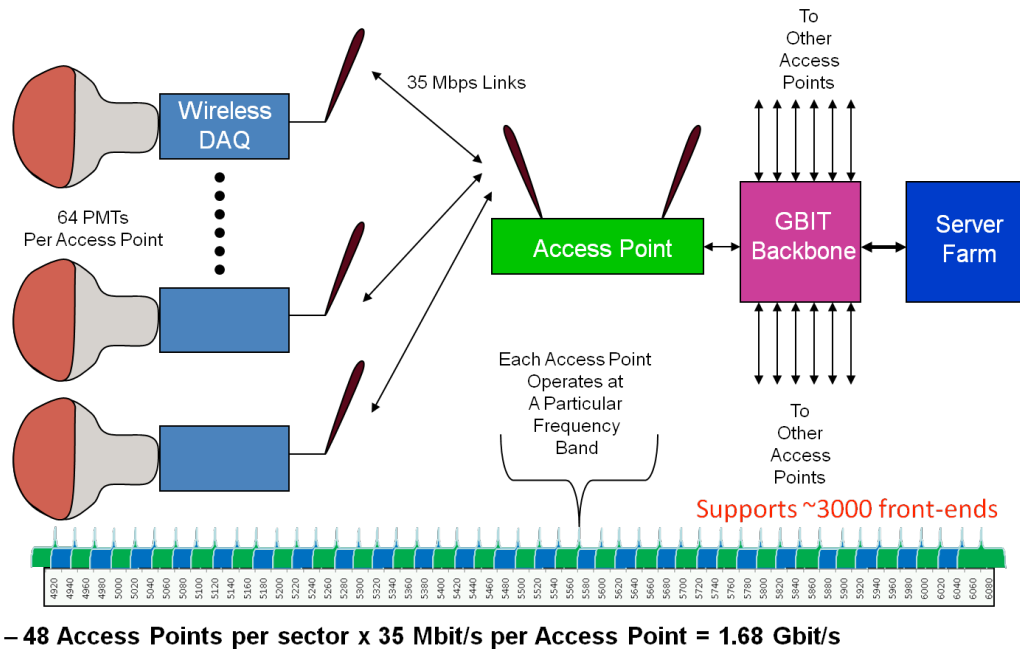


Figure 1: Allocation of frequency space for wireless data transmission.

total “sector” payload data rate of 7.68 Gb/s. The combination of these two extensions to this multi-access point concept should provide sufficient data throughput to read-out a large detector. Note that the above calculations do not account for latency in the communication. In practice, the latencies will impact the achievable throughput. In a real system, the DAQ system would probably have to poll the front-ends for data. This creates a defined handshake between client and access point and in principle increases latencies slightly but controls the readout process and avoids the need for clients requesting to send data. Ultimately this method increases the overall throughput. For our system, the intention is to have the server request data from each front-end with a periodicity of 1s.

2.2. Wireless Power Transmission

We tested both optical and RF power transfer methods. The optical demonstrator utilizes a high power light-emitting diode (LED) that is collimated into an 8 inch diameter beam and is received by a photovoltaic (PV) panel, as shown in Fig. 2. The LED used is an OSRAM SFH 4751 with 3.5 W optical output, operated at a maximum DC current of 1 A. The

LED wavelength is 940 nm which matches the peak efficiency of the Delsolar $156 \times 156 \text{ mm}^2$ photovoltaic cell used in our $312 \times 280 \text{ mm}^2$ PV panel array. Figure 3 shows the power received from this system as function of transmission distance. This test system met our prototype requirements of receiving 0.25 W at 5 meters.



Figure 2: Apparatus for optical power transmission. The LED and lens are inside the near tube, and the photovoltaic receiver is at the far end.

The RF power transfer test consisted of a function generator driving a 14 dBi gain Yagi antenna at 915 MHz with an output power of 10 dBm and being received by a 11 dBi gain patch antenna, as shown in Fig. 4. The measurements were taken in a large room at a significant height to minimize the scattering from surrounding objects. The data from these tests, as a function of transmission distance are shown in Fig. 5. The data points are in good agreement with the expectation from Friis transmission equation [10], which relates the ratio of power received P_r to power transmitted P_t for a

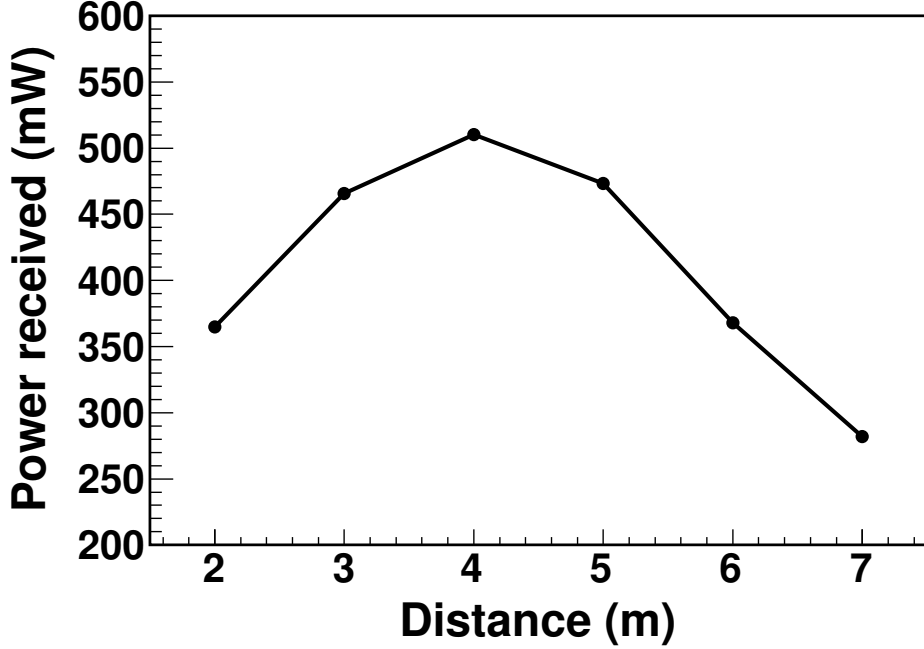


Figure 3: Power received (mW) by the photovoltaic panel as a function of distance (m) from the optical source. The optical source used was a 3.5 W LED with a 940 nm wavelength and a focusing lens.

given pair of antennas with gains G_t and G_r , operating at an wavelength λ , and separated by a distance R , as given in Eq. 1. There is a rapid fall off of received power as the transmission distance increases. At 5 meters the power loss is 20 dBm, which requires a 25 W source to receive 250 mW, our target power.

$$\frac{P_r}{P_t} = G_t G_r \left(\frac{\lambda}{4\pi R} \right)^2 \quad (1)$$

For this feasibility study, the optical system was the chosen prototype implementation. It provided a DC source that is relatively easy to utilize. RF power transmission requires converting the RF power into a DC supply, which is commercially available but only at a 100 mW receive power [11]. The optical power transfer system that we built met the power requirements for this demonstrator.

RF power could be a better choice for a large detector since one source

can power many front-ends. This greatly reduces the complexity and cost of the system. For example, at 5 meters the same power ± 3 dBm is being transmitted into a 2×2 m² area. For a 50 W output, a single equivalent source could power as many as 40 front-ends depending on the packing density.



Figure 4: Apparatus for RF power transmission. The RF transmitter (14 dBi gain Yagi antenna) is in the foreground, with the RF receiver (11 dBi gain patch antenna) at the far end.

3. Description of the Prototype System

Figure 6 shows a block diagram of the wireless demonstrator. The prototype system built is comprised of 4 boards that include: a board for generating high voltage for the PMT; a front-end board for shaping and digitization of the PMT signal; a digital board for processing the data and wireless data transmission; and a power board for receiving wireless power and generating

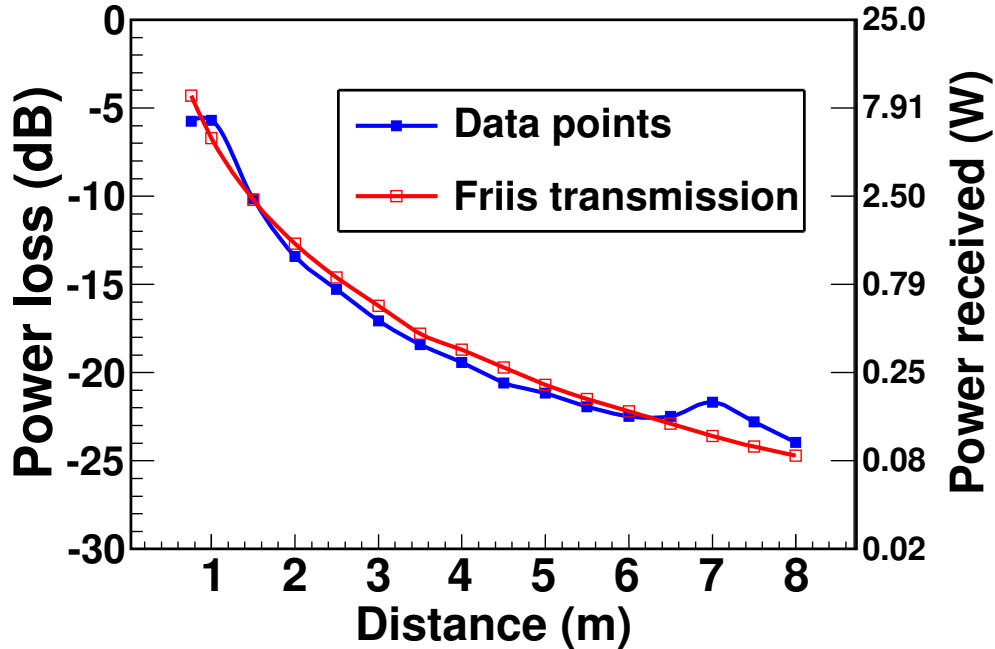


Figure 5: Power loss (dB) in the RF power transmission test as a function of distance (m) from the source. Solid dots are the measurements and open dots are the expectation from Friis transmission equation. The source is a 915 MHz 10 dBm transmitted through a 14 dBi gain Yagi antenna and received by an 11 dBi gain patch antenna. The scale on the right shows the power that would be received for a 25 W (44 dBm) source.

the different voltages needed by the system. The system was designed to connect to a photovoltaic panel and send data wirelessly using 802.11n in the 5 GHz band. Photos of the four boards in the PMT base are shown in Fig. 7. There is a power bus that connects the power PCB to the other three boards. A data bus connects the digital PCB to the front-end PCB and HV PCB. Physically they are arranged in the tube as shown in Fig. 8. The complete system with PMT is shown in Fig. 9.

3.1. Description of the Hardware

3.1.1. Power Board

The power board uses a LTC 3105 [12] switch mode step-up converter to turn the 1.85 V received from the photovoltaic panel into one of the system voltages, 5 V. The energy is stored in a series of ultra-capacitors [13] with an

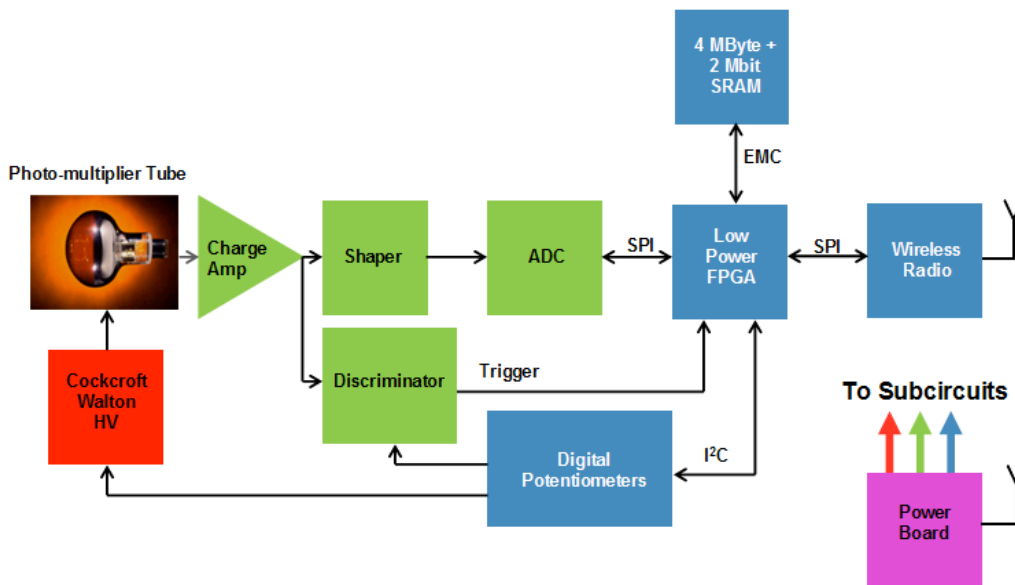


Figure 6: Block diagram of the wireless prototype system.

effective total capacitance of 2.5 F. The ultra-capacitors store energy locally and thereby reduce the peak power demand on the power system. The 5 V supply is used to generate 3.3 V, 1.8 V, and 1.5 V with LTC 3104 step-down convertors [14], and 24 V with a LT 3473 step-up converter [15]. The digital board uses 3.3 V, 1.8 V, and 1.5 V. The front-end board uses 3.3 V. The high voltage board uses 5 V and 24 V. The overall conversion efficiency of the power conversion, relative to the photovoltaic input, is 70%.

3.1.2. Digital Board

The digital board houses the processor, wireless radio, and other digital ICs (external low-power SRAM, SPI flash, etc.) The wireless radio used is a commercial board from ConnectBlue, the cBOWL221a [8]. It is an 802.11n single stream module with an SPI interface. This module was chosen because of its low power consumption. With a low latency SPI bus running at 50 MHz it supports a maximum payload transfer rate 35 Mb/s. The radio offloads all of the 802.11n protocol, but the TCP/IP or UDP/IP stack must be incorporated inside the processor. The digital processor used is a Microsemi A2F200 Smart Fusion [16]. It combines a 100 MHz hard ARM Cortex M3 processor, a relatively small FPGA, and includes 2 ADCs and

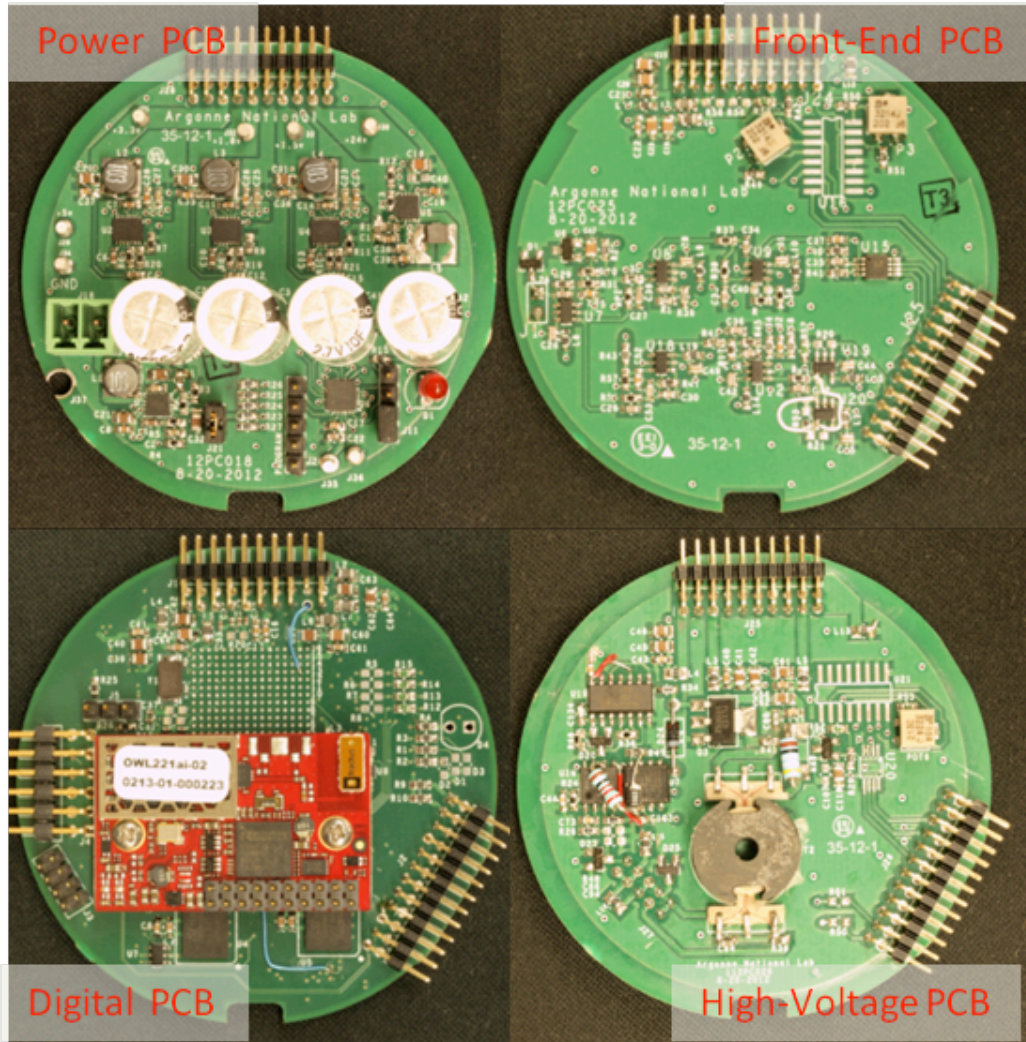


Figure 7: Pictures of the four printed circuit boards in the wireless prototype system. Upper left figure shows the power board, upper right shows the front end, lower left shows the digital and lower right shows the high voltage PCB.

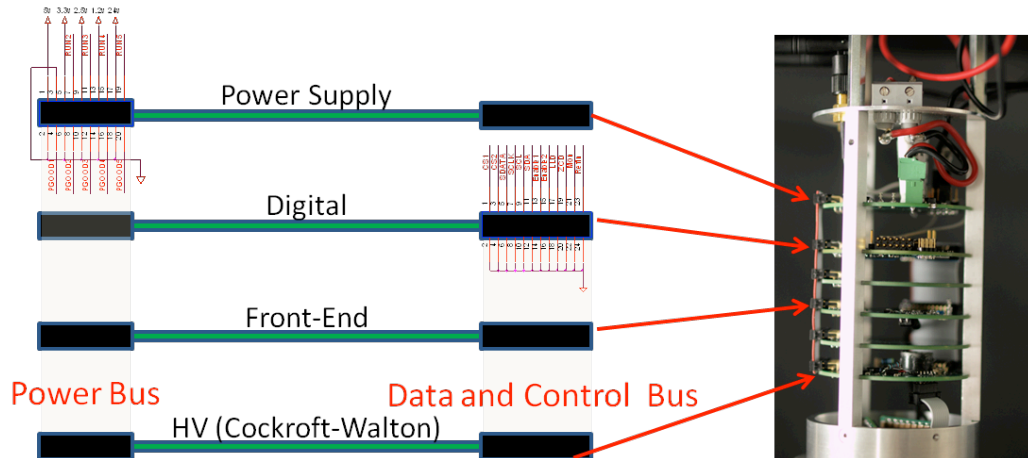


Figure 8: Partial assembly of the system with the PMT.

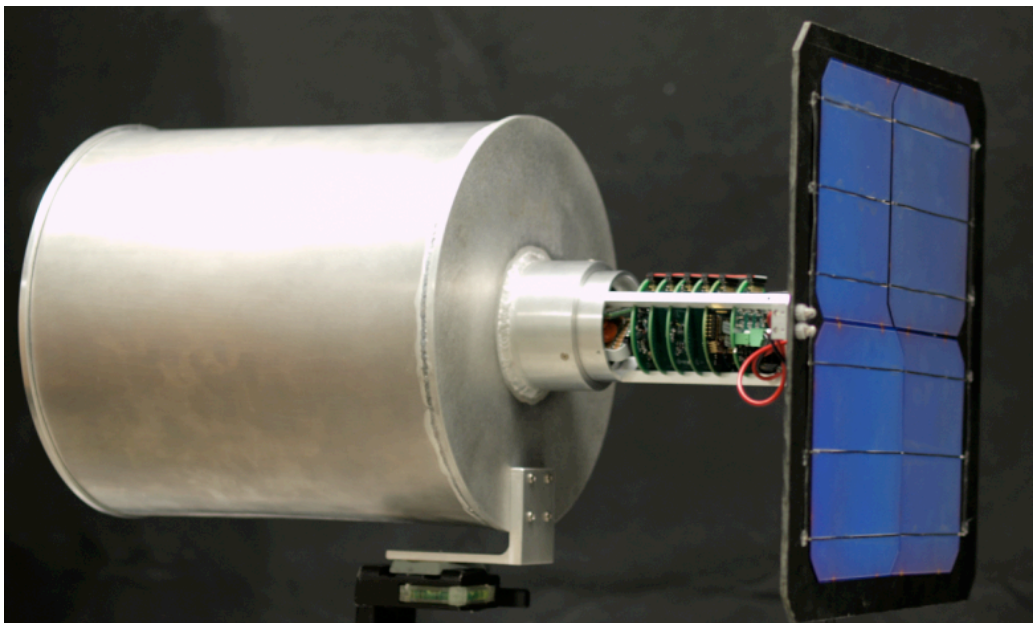


Figure 9: Picture of the completed system. Shown with light tight PMT enclosure and photovoltaic panel attached to a tripod (electronic enclosure open for reference).

2 DACs. The physical hooks to use the ADCs and DACs for readout and control are included in the design but have not been exercised. The driver code for the radio is provided by ConnectBlue. The version that we used is written for use with embedded Linux. We chose to use FreeRTOS [17] because of the low overhead and relative ease in adaptation of the provided OS based driver. While this reduced the effort required for driver integration, it made hardware interrupt handling difficult to incorporate, so this was not implemented. As a result, the processing of each frame could begin only after the last data had been transferred to the wireless module. This reduced the overall throughput rate. A non OS-based single task process would more easily handle hardware interrupts, reduce SPI bus latency, and reduce processor overheads. For a large system, this would provide better performance, at the expense of a longer development time. The FPGA fabric is used for the discriminator logic, ADC readout, time-stamping, and event word generation. It directly accesses the external memory and stores the events using the same memory controller as used by the processor.

3.1.3. High Voltage Board

The high voltage board uses a standard Cockcroft-Walton (CW) switching circuit to boost the 24 V input voltage up to 2000 V. The PMT is a 10-stage tube. Normally, the CW would have taps to connect directly to the dynodes. Unfortunately, the circuit was originally designed for a different PMT, and the change to the R7081HQE PMT made the connectivity incompatible. As a compromise, we implemented a resistive divider in the tube, but still retained the CW high voltage generation. While this worked acceptably, it caused the power consumption of the circuit to go up, as well as introducing rate limitations of the tube due to the relatively high values of resistance needed to make the circuit work. Nonetheless, we were able to run the circuit from wireless power, and the noise performance was sufficient to measure single photo-electrons.

3.1.4. Front-end Board

The front-end board includes a charge-sensitive preamplifier, shaping amplifier, programmable discriminators, and a 12-bit ADC. The output of the charge sensitive amplifier connects to both a uni-polar and a bi-polar shaping amplifier. The uni-polar shaping amplifier connects to the AD7451 ADC [18] and is used for digitizing the pulse-height. The bi-polar shaping amplifier is used as the input to pair of comparators, one of which is used for pulse-height

Table 2: Summary of initial goals and achieved performance for the wireless data acquisition system.

Specification	Target	Performance
Total power consumption (@ 10 kHz)	250 mW	386 mW
Digital	120 mW	216 mW
Front-end	30 mW	39 mW
HV	80 mW	131 mW
Maximum event rate	10 kHz	80 kHz
Data transfer rate	35 Mb/s	11 Mb/s
Bit Error Rate	$< 1 \times 10^{-12}$	Dropped Packets

discrimination and the other for timing. The comparator outputs connect to the A2F200 FPGA fabric (digital board) over the data and control bus. As discussed, the A2F200 FPGA fabric is used for the discriminator logic to control the ADC readout.

3.2. Readout System and Process

The prototype readout system is shown in Fig. 10. It consists of a Linux computer running Scientific Linux [19] and a commercial access point, a Cisco E3000 [20] running DD-WRT firmware. The readout code was written to receive and store incoming UDP packets. For each asynchronous PMT trigger the pulse height and time stamp are stored. Once per second the front-end transmits the data as a single UDP packet to the server. A program running on the server receives and stores the UDP packets. Currently only data push from the front-end is implemented. As mentioned in section 2, implementing data pull is critical to extract the maximum throughput from multiple front-ends in a large detector.

4. Performance

The prototype system described above has been built and tested. It is powered wirelessly using the optical source received by the photovoltaic panel. All of the tests discussed here were performed with the system running from wireless power. The performance achieved is summarized in Table 2.

The power consumption of the system is 386 mW, higher than the initial 250 mW target. The primary causes of the increase are in the digital and the high voltage boards. In the case of the digital board, the target specification

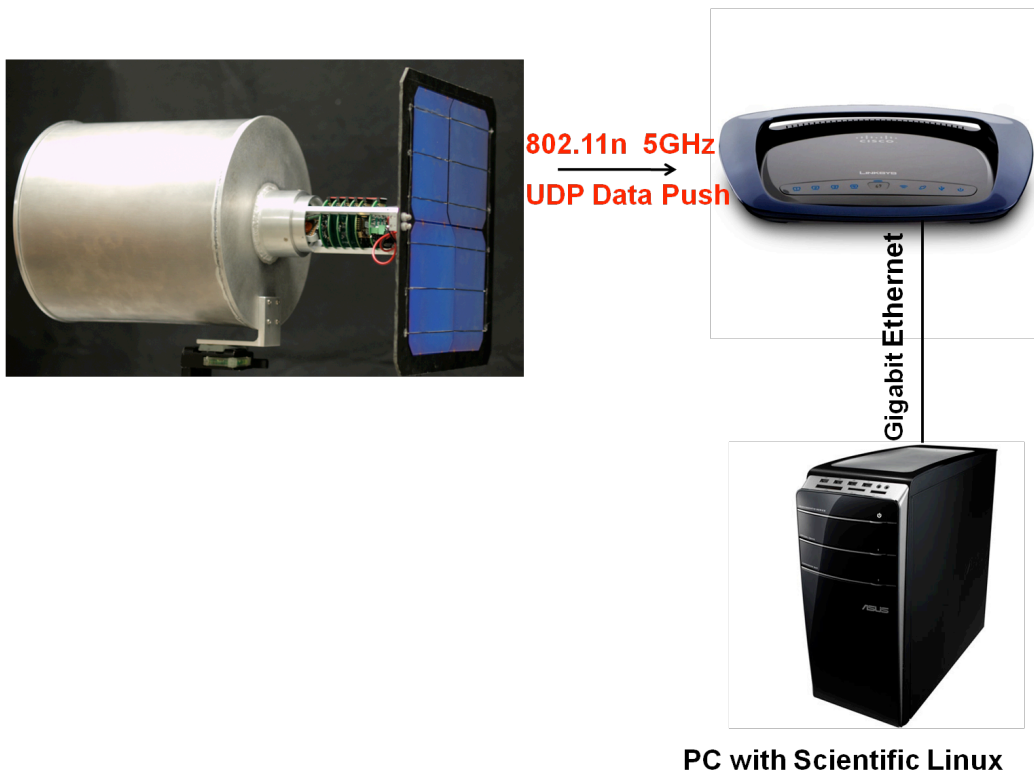


Figure 10: Configuration of the prototype readout system.

was based on spreadsheet power estimator, which does not accurately reflect actual operation. The high voltage board had to use a resistive divider as described earlier. Both of these problems are understood, and we feel that the original targets can be achieved in the next version of the design. The system is capable of sending greater than 10k events/s (60 kB/s). However, the critical parameter for performance in a large detector is the maximum burst transfer payload data rate. The specification of 35 Mb/s is the maximum transfer rate of an 802.11n single stream link, and this was our target. While this is achievable with the cBOWL221a radio, it does necessitate zero SPI bus latency and a 50 MHz SPI clock. The maximum burst transfer rate that we achieved was 11 Mb/s. The reason for this was twofold. First, the maximum SPI clock rate in the SmartFusion A2F200 is set by the master clock divided by 4. This limits the maximum SPI clock rate to 25 MHz. Second, latencies caused by FreeRTOS, the driver code, and the speed of the A2F200 processor, account for the remaining difference. The pin-compatible A2F500 supports a 50 MHz SPI clock and will be implemented in the future. This simple change should yield 18 Mb/s. Reducing the latency would require the elimination of FreeRTOS and driver optimization, as discussed earlier. Our target bit error rate (BER) was less than 1×10^{-12} . A bit error rate test (BERT) program was written to analyze the performance. The prototype system has been run for many hours at a time with no bit errors observed in any received packets. This is due in part to operating a relatively simple system, one broadcaster at a time, in the largely unused 5.5 GHz band in our lab. It is also due to the forward error correction that is incorporated in the 802.11n protocol. However, significant numbers of dropped packets were observed, on the order of 1 in 2000. It is believed that this is due to the use of UDP. While more efficient than TCP, UDP does not have guaranteed transmission. We traced the problem to our access point, having observed the drop packets with the same frequency by using a computer to generate fake data. It may be possible to significantly reduce the systematic packet loss. The nature of UDP will require some consideration of error detection and recovery for a large system.

We have collected data with the prototype system operated from wireless power and with wireless data readout. The front-end circuit exhibits very low noise, which is clear from the pedestal data in Fig. 11. The integral linearity over the full digitization range is quite good, better than 0.4%, as shown in Fig. 12. To test the data acquisition capability, a sodium iodide crystal was attached to the PMT and tested with ^{241}Am (Fig. 13) and ^{137}Cs

(Fig. 14) sources.

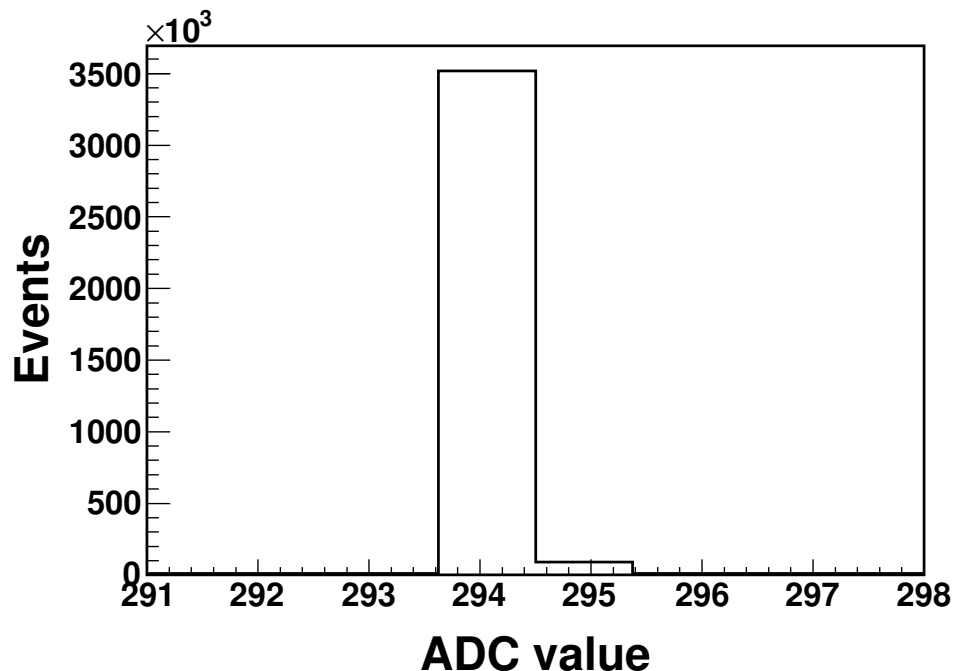


Figure 11: Measurement of pedestal. The system is operated with conditions 10k events/s, self-triggered, HV on with no PMT, system powered wirelessly and wireless readout.

5. Summary

We successfully designed and built a wireless data acquisition system implemented in a photomultiplier tube base that operates from wireless power and sends data wirelessly. The power consumption, while slightly greater than our target, is still low enough to allow the system to operate from our optical power transfer system. The use of the pin-compatible A2F500 SmartFusion device should increase the burst transfer rate from 11 Mb/s to 18 Mb/s. Assuming 480 Kb/s average data rate from our front-ends and assuming a conservative estimate of the latency between request for data and transmission of data of 10 mS, the burst transfer rate achieved would support 18 and 27 front-ends for 11 and 18 Mb/s respectively. A system with 48 access points would support 1296 front-ends. Our future effort will

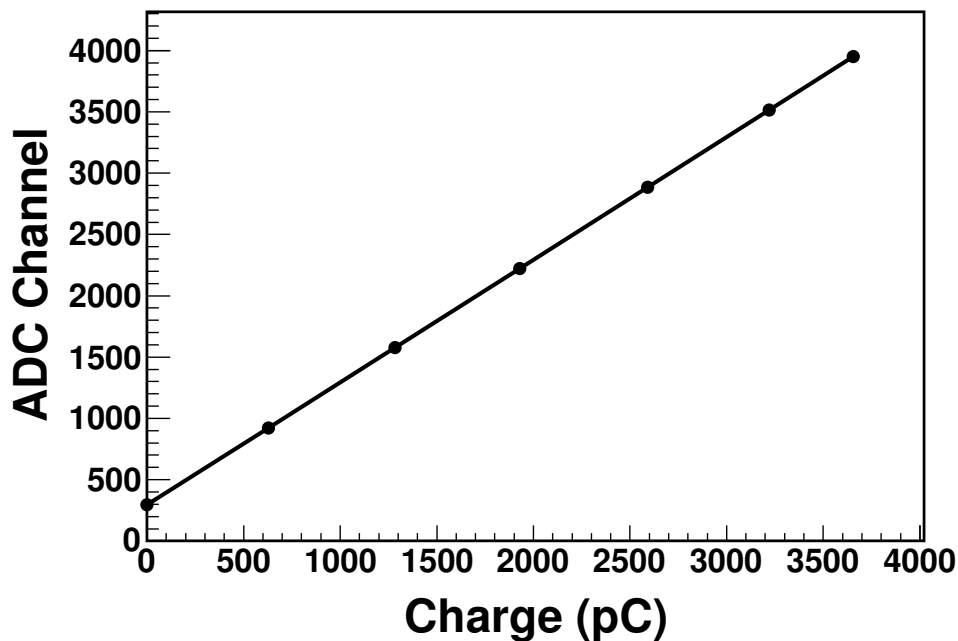


Figure 12: Response from electronic charge injection. The system is operated with conditions self-triggered, PMT HV on, system powered wirelessly and wireless readout.

address the SPI clock rate issue by using the A2F500, eliminating FreeRTOS, and reducing the SPI bus latency. This should reduce power consumption in the digital board. The high-voltage board will be redesigned to integrate correctly into the chosen PMT. In the longer-term, the intention is to use RF power transfer to facilitate the simplification of using one transmitter to power many receivers. Investigating the use of a custom ASIC for lower power operation of the front-end and Cockroft-Walton control circuitry would also be considered for a larger system.

6. Acknowledgments

We acknowledge the support of Laboratory Directed Research & Development from Argonne National Laboratory to carry out this project. We would also like to thank Jeff Maus and Henric Lindn of ConnectBlue for supporting our efforts to incorporate the cBOWL221a 802.11n wireless radio

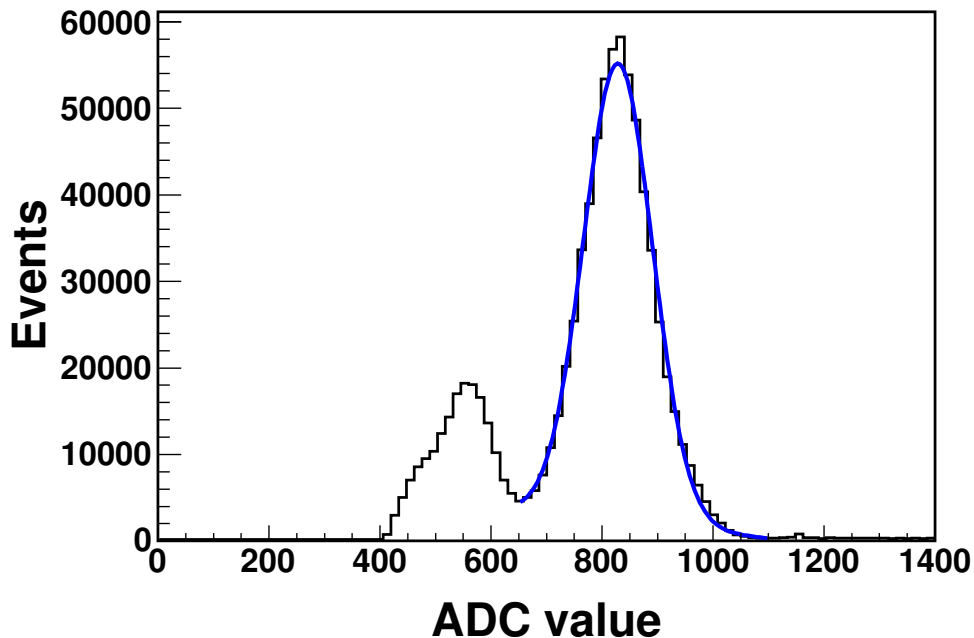


Figure 13: Response from 60 keV ^{241}Am source. The system is operated with conditions 1k events/s, self-triggered, PMT HV 1300V, system powered wirelessly and wireless readout.

working in our system. We especially thank Greg Mears of the Microsemi Corporation for his help with the SmatFusion system-on-chip device.

References

- [1] R7081-02 Datasheet, Nov. 12. 2003, Hamamatsu Photonics K.K., 325-6, Sunayama-cho, Naka-ku, Hamamatsu City, Shizuoka Pref., 430-8587, Japan.
- [2] T. Akiri et al., The 2010 Interim Report of the Long-Baseline Neutrino Experiment Collaboration Physics Working Groups, arXiv: 1110.6249.
- [3] D. Autiero et al., Large underground, liquid based detectors for astro-particle physics in Europe: scientific case and prospects, arXiv: 0705.0116.

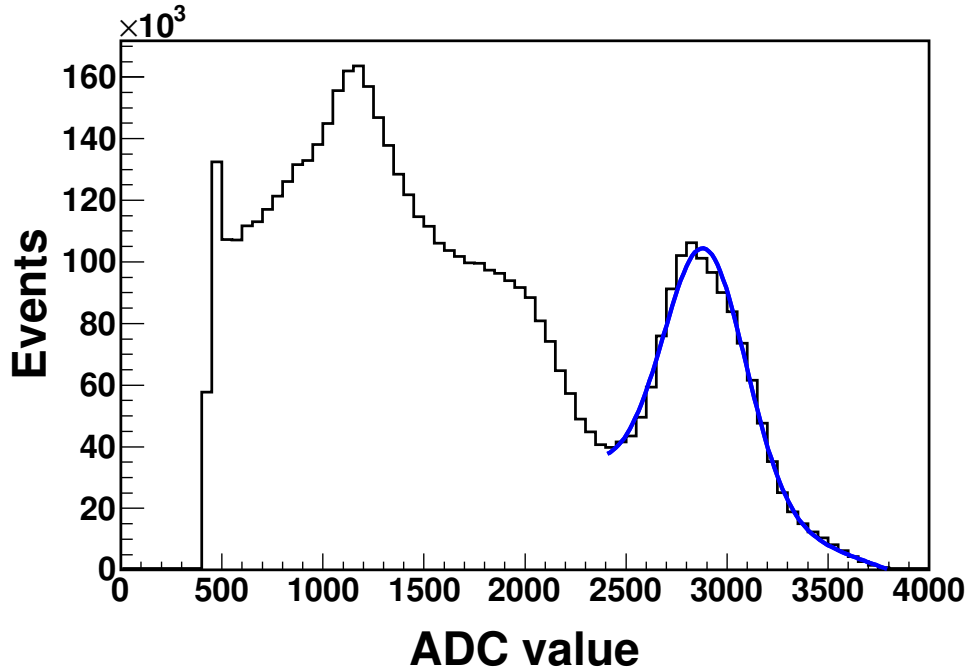


Figure 14: Response from 661.7 keV ^{137}Cs source. The system is operated with conditions 250 events/s, self-triggered, PMT HV 1200V, system powered wirelessly and wireless readout.

- [4] K. Abe et al., Letter of Intent: The Hyper-Kamiokande Experiment-Detector Design and Physics Potential, arXiv:1109.3262.
- [5] P. Adamson et al., CHerenkov detectors in mine PitS (CHIPS): Letter of Intent to FNAL, arXiv:1307.5918.
- [6] A. Kurs, *et al.*, Science **317**, 83 (2007).
- [7] P. De Lurgio, W. Fernando, B. Salvachua, R. Stanek, D. Underwood, D. Lopez, “New Optical Link Technologies for HEP Experiments”, in Proc. DPF-2011 Conference, Providence RI, August 8-13, 2011.
- [8] cBOWL221a Product Brief, cBProduct-0811-01 (1.6), Aug. 2011, ConnectBlue AB, Norra Vallgatan 64 3V, SE-211 22 Malmö, Sweden.
- [9] Part 11: Wireless Lan Medium Access Control (MAC) and Physical Layer (PHY) Specifications, IEEE Standard 802.11TM-2012.

- [10] H. T. Friis, "A Note on a Simple Transmission Formula", Proceedings of the IRE., vol. 34, no. 5, pp. 254 - 256, May 1946.
- [11] P1110 915 MHz RF PowerharvesterTM Receiver Datasheet, Rev A, Apr. 2010, Powercast Corporation, 566 Alpha Drive, Pittsburgh, PA 15238, United States.
- [12] LTC3105 Datasheet, 3105fa Rev A, Feb. 2011, Linear Technology Corporation, 1630 McCarthy Blvd., Milpitas, CA 95035, United States.
- [13] ESHSR-0010C0-002R7 Datasheet, (446-901) 750-8, Gomae-dong, Giheung-gu, Yongin-si, Gyeonggi-do, Korea.
- [14] LT3104 Datasheet, 3104f, Oct. 2011, Linear Technology Corporation, 1630 McCarthy Blvd., Milpitas, CA 95035, United States.
- [15] LT3473 Datasheet, 3473f, Feb. 2005, Linear Technology Corporation, 1630 McCarthy Blvd., Milpitas, CA 95035, United States.
- [16] SmartFusion Customizable System-on-Chip (cSoC) Datasheet, Rev 9, Sept. 2012, Microsem Corporation, One Enterprise, Aliso Viejo CA 92656 United States.
- [17] FreeRTOS, Available: <http://www.freertos.org>.
- [18] AD7451 Datasheet, C03153-0 Rev. C, Mar. 2007, Analog Devices, 3 Technology Way, Norwood, MA 02062, United States.
- [19] ScientificLinux, Available: <http://www.scientificlinux.org>.
- [20] E3000 Datasheet, 10031010NC-JL, Oct. 2010, Cisco Systems, Inc., 170 West Tasman Dr., San Jose, CA 95134, United States.